Eastern equatorial Pacific warming delayed by aerosols and thermostat response to CO2 increase

Ulla K. Heede, Alexey V. Fedorov

Eastern equatorial Pacific warming delayed by aerosols and thermostat response to CO_2

Ulla Heede (ulla.heede@yale.edu)
Yale University https://orcid.org/0000-0002-3241-0552
Alexey Fedorov
Yale University

Article

Keywords: global warming, east-west temperature gradient, Walker circulation

Posted Date: January 12th, 2021

DOI: https://doi.org/10.21203/rs.3.rs-133479/v1

Version of Record: A version of this preprint was published at Nature Climate Change on July 29th, 2021.
See the published version at https://doi.org/10.1038/s41558-021-01101-x.

Abstract

Understanding the tropical Pacific response to global warming remains a challenging problem. Here, we assess the recent and future evolution of the equatorial Pacific east-west temperature gradient, and the Walker circulation, across a range of different greenhouse warming experiments within the CMIP6 dataset. In abrupt CO_2-increase scenarios many models generate an initial strengthening of this gradient resembling an ocean thermostat (OT), followed by a small weakening; other models generate an immediate weakening that becomes progressively larger establishing a pronounced eastern equatorial Pacific (EP) warming pattern. The initial response in these experiments is a very good predictor for the future EP pattern simulated in both abrupt and realistic warming scenarios, but not in historical simulations showing no multi-model trend. The likely explanation is that recent CO_2-driven changes in the tropical Pacific are masked by aerosol effects, and a potential OT delay, while the EP warming pattern will emerge as greenhouse gases overcome aerosol forcing.

Main Text

Understanding the emerging warming patterns in the tropical Pacific holds several keys to understanding how the Earth's climate responds to increasing levels of greenhouse gases [1–4]. This is true on interannual timescales, as changes in El Niño - Southern Oscillation (ENSO) are intrinsically linked to changes in the tropical Pacific mean state [5–7] and on decadal and longer timescales, as slow variations in the strength of Pacific trade winds and ENSO modulation can explain the periods of temporary slowdown of global warming trends [3,8–11] with links to climate sensitivity [12,13]. At these different timescales, the tropical Pacific warming modulates atmospheric tropical circulation, rainfall[14], and teleconnections to mid-latitudes[15,16]. Therefore, it is imperative to understand and predict changes in the tropical Pacific (or more generally the Indo-Pacific), yet progress has been hindered by discrepancies between the observed and modelled trends[17], diverging theories[1], and uncertainties in future projections[18]. Accordingly, our goal is to investigate these changes and reconcile the lingering discrepancies using a broad array of realistic and idealized warming experiments of the Climate Model Intercomparison Project Phase 6 (CMIP6).

Recent studies demonstrate that Pacific surface winds, sea surface temperature (SST) and sea level pressure (SLP) gradients along the equator have increased over the satellite era [14,19–21]. Furthermore, the Indian Ocean has been warming at a faster rate than the Pacific since the 1950s [22,23]. Whether these trends are driven by anthropogenic climate change remains under debate. Clement et al.[24] proposed a mechanism by which the Pacific SST gradient may increase in response to atmospheric warming, as the surface water in the western Pacific warms faster than the upwelling-cooled water in the east. This effect, dubbed the 'ocean thermostat' (OT), has been demonstrated as a transient response in box models [25] and several ocean GCMs [26,27]. In the latter case, the OT typically involves a central, rather than eastern Pacific cooling; consequently, the Indo-Pacific temperature contrast increases with a CO_2 rise, but the effect eventually reverses after decades to a century [27]. The potential importance of inter-basin warming

contrasts in driving the Pacific cooling[11] is also documented in experiments imposing SST changes in the Indian and Atlantic oceans [9,23,28,29]. In addition, off-equatorial wind-evaporative-SST (WES) feedbacks in the Pacific trade wind belts may further contribute to the OT effect and the lack of warming in the tropical central and eastern equatorial Pacific [30].

While the observations have shown a strengthening of the Pacific east-west SST gradient in the satellite era, in future forcing scenarios the majority of GCMs archived in the previous model intercomparison (CMIP5) predicted a weakening of the zonal SST gradient [17,18], associated with the formation of the eastern equatorial Pacific (EP) warming pattern. Several mechanisms have been proposed to explain this SST gradient weakening, including enhanced evaporative damping over the warm pool [31], increased static stability and slowdown of the ascending branch of the Walker circulation [32], low cloud feedbacks [33] and warming of the extra-tropical regions that provide source water for equatorial upwelling [27,34]. However, the robustness of this weakening has been questioned due to the inability of the CMIP5 models to capture the observed tropical Pacific trends [17,35], a large spread in the projected future changes [18], GCM biases in SST and winds along the equator [36,37] and deficiencies in simulated ENSO [38,39]

Here we utilize the CMIP6 archive - a new chapter in climate model development, to address these outstanding challenges using an updated and expanded collection of GCMs with new forcing scenarios, which enables a better assessment of both historical and future trends, offering new insights into the drivers of inter-model and observation-model discrepancies in the tropical warming patterns with implications for future projections.

Temporal evolution of the tropical Pacific response to global warming

We investigate the warming pattern in the tropical Pacific and Indian Oceans across several types of CMIP6 model experiments, from abrupt CO_2 increase to realistic scenarios forced by different concentrations of greenhouse gases (GHGs) and aerosols. To fully capture the observed and simulated trends [23,27,40], we define the equatorial east-west SST gradient as the surface temperature over the Indo-Pacific warm pool region minus the central-east Pacific temperature (Methods). We will consider the time evolution of this Indo-Pacific gradient in a multi-model mean sense, and in parallel discuss inter-model differences.

All but one model show a long-term weakening of this gradient across the future projections and abrupt CO_2-increase experiments (Fig1b-e). However, in the historical full-forcing experiment, the models show no significant trend on average (Fig 1a), albeit with a significant inter-model spread (Fig 1a, also Fig 5). In other words, the long-term changes in the tropical Pacific appear to be disconnected from the historical simulations. Potentially, this delayed response can be caused by two major factors. The first factor is the competition between the ocean thermostat effect and the opposing atmospheric and oceanic mechanisms that act to weaken the Pacific zonal temperature gradient in response to CO_2-forcing. The other factor is the effect of aerosol emissions , which can influence the warming patterns in the tropical

Pacific [41,42] and delay the expected weakening of the east-west temperature gradient. We will explore these two factors separately, first examining hypothetical CO_2-only scenarios, then analyzing realistic full-forcing historical and future Shared Social Pathway (ssp) scenarios with both aerosol and GHG-forcing, and finally analyzing a subset of models wherein we can separate the aerosol and CO_2 effects.

Ocean thermostat and EP warming pattern in CO_2-forced experiments

Taken together, the CO_2-only simulations show a small transient strengthening of the equatorial Pacific temperature gradient lasting about 10 years for the abrupt CO_2 experiment, and no initial change over 50 years followed by a delayed weakening for the gradual 1pct forcing (Fig 1d-e). Thus, depending on how abruptly the system is perturbed and the model in question, the long-term weakening response of the zonal temperature gradient can be indeed delayed by a transient strengthening or an initially flat trend in response to CO_2-forcing.

To understand these initial (transient) changes and the spread between the models, we separate models based on their initial response in the abrupt CO_2-forcing experiments and extract two end-member categories (see the legend of Fig 4). The ocean thermostat category (OT) contains 7 models which are characterized by a strong transient response (above 0.25 K increase in the temperature gradient) for the first 25 years. The eastern equatorial Pacific warming (EP) category contains 13 models that exhibit an immediate weakening of the gradient (below -0.25K) in the first 25 years. The rest of the models fall in between these end-members.

The initial response of the OT category is characterized by cooling anomalies in the central equatorial Pacific as well as south-east Pacific (Fig 2a) and an anomalous pressure gradient between the Indian and Pacific Oceans (Fig 3a). Note that in order to highlight the spatial pattern of temperature change, we subtracted the mean warming signal over the region. The lack of warming in the eastern and central Pacific can be explained by continuous upwelling of cold water that balances the CO_2-induced radiative forcing, while the western equatorial Pacific and the Indian ocean, along with the Maritime continent, warm at a faster rate. This sets up an anomalous equatorial Indo-Pacific pressure gradient, strengthening local winds and leading to a transient cooling [26,27] in the central and parts of eastern equatorial Pacific (Fig 2a). The off-equatorial wind-evaporation-SST (WES) feedback [27,30,43] further strengthens the trade winds south of the equator (Fig 3a), contributing to the lack of warming in the central and eastern Pacific.

The surface warming patterns are very different in the EP category, which instead show a broad warming from the eastern to central Pacific (Fig. 2c) and associated low pressure anomalies there (Fig 3c). Such changes are thought to be related to strong low-cloud feedbacks [44,45] in response to the CO_2 forcing, causing eastern Pacific marine boundary layer cloud cover to reduce, which in turn increases warming at the ocean surface and weakens the Walker circulation (Fig 3c).

While the two categories of models are vastly different in their initial response, they converge eventually to a warming pattern characterized by an enhanced eastern equatorial warming [45,46], with a sharp meridional contrast especially in the southern hemisphere (Fig 2b and 2d). The magnitude of this pattern is, however, still much weaker in the OT category. The transition from cooling to warming (OT models) or the strengthening of warming (EP models) in the eastern Pacific can be explained by the gradual warming of the upper ocean, which reduces the effect of the ocean thermostat. This allows other competing mechanisms, such as decreased vertical mass flux over the warm pool [32], enhanced evaporative damping in the west, and enhanced extra-tropical warming to become dominant, leading to slowdown of the Walker circulation [27,47]. In the EP category, these mechanisms, in addition to the cloud feedbacks, allows for a greater Walker circulation slowdown and a broader equatorial warming.

Thus, the structure, magnitude and the timing of emergence of the Pacific warming pattern are controlled by the competition between the ocean thermostat versus the eastern Pacific warming effects [27,46]. The balance between these mechanisms appears to be related in part to mean state differences between the models – on average, the OT models are colder, including the warm pool, and have stronger south-easterly and north-easterly Pacific trade winds than the EP category (Fig S2). Stronger off-equatorial winds favor the WES feedback, strengthening the OT-response, whereas a colder warm pool may reduce evaporative damping, weakening the EP-response.

While most models do exhibit the transient strengthening of the temperature gradient in the first 10 years of the abrupt CO_2-increase experiment (Fig 1a), only several show a particularly strong change, exceeding +0.2 K and lasting up to 25 years (Figs 4a and 5a). These latter models have a particularly small magnitude long-term response. On the contrary, models that do not display the transient ocean thermostat have a much stronger long-term EP warming. Overall, initial and long-term changes in the temperature gradient in the abrupt forcing experiments are highly correlated (Fig. 4a). Furthermore, long-term changes in the gradual 1pct simulation are highly correlated with the initial changes in the abrupt experiments by the same models (Fig. 4b). In 1pct experiments, the OT models also show the longest delay (up to 80 years) in weakening of the gradient.

Thus, despite some inter-model spread, the initial response in the abrupt CO_2 forcing experiments gives a very good prediction of the strength of the long-term EP warming across hypothetical CO_2 scenarios and, as discussed next, it is also a very good predictor for the long-term response in realistic ssp experiments and the trends in historical simulations forced only by CO_2.

Full-forcing historical and future projections

Similar to the 1pct CO_2-only experiments, realistic ssp scenarios show a high correlation between the long-term response of the zonal temperature gradient and the initial response in the 4xCO_2 abrupt experiments (Fig 4e,f). This is the case both for the ssp858 scenarios, in which aerosol emissions decline rapidly, and the ssp730 scenario, which maintains aerosol emissions close to the level of 2000-2010 [48]. Consequently, in the long-term tropical Pacific response, CO_2 and other GHGs dominate over aerosols,

and again the characteristics of the initial response in the abrupt 4xCO_2 experiments define long-term changes.

In contrast, we find no correlation between historical simulations and the initial response in the abrupt-forcing experiments (Fig. 4d). This could be because in the historical experiments GHG changes are relatively low, compared to abrupt 4xCO_2 or 1pct CO_2, and hence natural variability dominates the signal [49]. However, 4-5 models show a significant ensemble-mean strengthening of the Pacific SST gradient for the recent decades (Fig 5b) that is consistent with observations and yet inconsistent with CO_2-only scenarios for the same models. On the contrary, for 14 models with GHG-only historical runs available, the correlation between the simulated historical trends and the initial response in the 4xCO_2 experiments is quite high (0.73 versus 0.18 for the full historical forcing, Fig. 4c). In other words, without aerosols, these models would predict trends for the past 60 year – from flat to a substantial gradient weakening – that are consistent with the initial respone in the 4xCO_2 experiments. This suggests that aerosol effects can strengthen the SST gradient temporarily or delay its weakening, which, in addition to noise caused by natural variability, causes the correlation between historical simulations and abrupt CO_2-only experiments to break down.

Opposing aerosol and GHG effects

To investigate further how aerosols modulate the tropical Pacific response to global warming, we have analyzed a subset of 12 models for which two complementary simulations are available: historical GHG-only and aerosol-only experiments. For these models, we can compare mean changes in surface temperature and pressure patterns in the full-forcing historical simulations to these hypothetical partial-forcing experiments. We focus on the changes since the 1950s where reliable measurements of both the radiative forcing and global temperatures are available.

The full-forcing historical simulations show an enhanced warming over land with stronger warming over the continents at mid to high latitudes but less warming over South Asia. The patterns of change over the ocean are much more muted, with only a hint of warming in the equatorial east Pacific (Fig. 6a). Likewise, while the SLP and wind anomalies show significant changes in the extra-tropical Pacific and the Indian ocean (the latter effect is likely related to aerosol emissions over Asia), the anomalies are small in the equatorial Pacific with only weak signature of westerly wind anomalies in the east. This relatively weak response contrasts the the GHG-only historical simulations, whose multi-model-mean warming pattern looks similar to the EP warming pattern in the 4xCO_2 experiments, and is characterized by a clear equatorial warming signal in the eastern and central Pacific and anomalous wind convergence towards a negative SLP anomaly off South America.

In contrast, the aerosol-only model-mean historical simulation shows a clear equatorial cooling signal, albeit of a smaller magnitude. The pattern looks similar to an EP pattern but of opposite sign. Unlike the OT-type response, this cooling is not accompanied by low pressure anomalies over the Indian ocean. Instead, low pressure anomalies develop over the southern Pacific and western Atlantic and weak positive

anomalies develop along the equator, leading to an anomalous equatorial divergence of winds especially pronounced in the southern hemisphere.

In the model-mean sense, the aerosol and GHG forcings appear to produce opposite trends in the tropical Pacific and therefore largely cancel each other in the historical simulation, forming a muted warming pattern. Nevertheless, individual models within this subset reveal large inter-model differences. These differences include the overall temperature sensitivity to aerosol and GHG forcings, the extent to which aerosols cause a patterned versus uniform cooling, and whether the response to aerosols and GHG-forcing is linearly additive or subject to nonlinear interaction. To illustrate these differences, we analyze three models in more depth (Fig S3). The HadGEM3-GC31-LL model stands out because it has a stark contrast between the full-forcing historical experiment, which generates a central equatorial Pacific cooling of similar magnitude as the observations, and the GHG-only historical experiment, which shows a clear EP warming. This contrast is probably driven by nonlinear interaction between aerosols and GHG forcings, since a linear superposition of the aerosol and GHG-only simulations does not produce equatorial cooling (Fig S4).

Several other models, notably CESM2-FV2, TaiESM1 and UKESM1, generate a strong SST gradient strengthening in the historical simulations, but do not show an OT-type response in CO_2-only scenarios (Fig 5). Similar to HadGEM3-GC31-LL, these historical trends might be driven mainly by aerosol forcing and nonlinear aerosol-GHG-interaction, rather than the OT mechanism.

Two other models, MIROC6 and CNRM-CM6, show generally similar warming patterns between the historical full-forcing and GHG-only simulations, and are less sensitive to aerosol forcing than HadGEM3-GC31-LL (Fig S4). Yet, CNRM-CM6 develops a slight equatorial cooling response in both the GHG-only and full-forcing scenarios (Fig S5), while MIROC6 has a slight eastern Pacific warming trend in the full-forcing simulation, and a clear eastern Pacific warming trend in the GHG-only simulation (Fig S6). Thus, CNRM-CM6 is representative of the models that show a gradient strengthening or no trend in the historical simulations due a delay of EP warming likely driven primarily by an OT-type response with aerosol effects superimposed, while MIROC6 may represent models that show a slight weakening of the gradient in the full historical experiments since they do not have strong aerosol or OT-type effects, and thus generate historical trends opposite to the observations.

Discussion

We have investigated the response of the tropical Pacific to climate change across a range of warming experiments from the CMIP6 dataset. Focusing first on abrupt 4xCO_2 experiments, we distinguish two types of model behavior based on the initial (decadal) changes – (1) models with a relatively strong OT-like initial response followed by a weak and delayed eastern equatorial Pacific warming and (2) models in which an EP warming starts to develop within the first few years. Eventually, nearly all of CO_2-only experiments (abrupt, 1pct gradual, partial-forcing historical) develop an EP warming but of vastly different magnitudes, and the initial response in the 4xCO_2 experiments provides a very good predictor for

the eventual strength of the EP pattern. The initial OT-like response is followed by a weak long-term EP pattern, while the initial, relatively weak EP pattern develops into a strong EP pattern. Across the models, the correlation between the initial $4xCO_2$ and longer-term changes of the Pacific zonal temperature gradient in different types of experiments varies from 0.73 to 0.86. This confirms the high utility of abrupt $4xCO_2$ experiments in elucidating the physics of the response and highlighting the competition between the OT and EP mechanisms.

Despite the strong correlation between the initial and long-term responses across CO_2-only experiments, we find no correlation between $4xCO_2$ experiments and the historical simulations. By analyzing a subset of models in which we can separate the effects of aerosols and GHGs, we show that this poor correlation is likely accounted for by the effect of aerosols, which act to counter the GHG warming pattern and thus suppress or delay the EP warming response in the full-forcing experiments. A relatively strong OT effect in some of the models is another factor contributing to this delay.

In future scenarios with growing GHG concentrations, even with continued aerosol emissions, the eastern equatorial Pacific warming becomes more pronounced and its magnitude starts again to correlate very well with the $4xCO_2$ initial response, as the GHG-driven tropical response overcomes aerosol effects. Thus, ultimately, our results suggest that any anthropogenic component of current observed trends in the tropical Pacific is of transient nature, and caused by either aerosol effects or an ocean thermostat type response to GHG-forcing, or a combination of both, acting to delay the EP warming. Consequently, as future atmospheric GHG concentrations increase further, and aerosol emissions level off or reduce, we may expect an enhanced warming of the eastern equatorial Pacific and associated weakening of the Walker circulation.

These findings raise a number of key questions. First, the large spread in long-term projected future changes to the tropical Pacific is still an issue in CMIP6, and it appears to be caused by inherent differences in how the models respond to CO_2 rather than aerosol effects or natural variability. The competition between various mechanisms that seek to either strengthen or weaken the Pacific temperature gradient, including the transient ocean thermostat effect, play out differently in each model, and how these differences are related to model biases, and cloud and convective parameterizations remains a challenging question to address. A generally colder tropical Pacific and stronger north-easterly and south-easterly trade winds seem to favor the OT effect, but with large variations across the models.

Second, very few models appear to capture the historical observed trend, whether aerosol driven or not, and even among those models differences in controlling mechanisms, and in future projections, are large. If aerosols are indeed driving the observed lack of warming in the equatorial central and eastern Pacific, one may expect a strong reversal of this trend once aerosol emissions level off and GHG effects take over. However, if the observed trends in the Pacific are driven primarily by an OT-type response, perhaps in combination with multi-decadal natural tropical variability, we may expect a delayed and weaker EP warming pattern. The uncertainty in what drives the observed trend thus makes it difficult to obtain more

robust projections of future trends, warranting more scrutiny of the role of aerosols in the models and constraints on the relative strength of the transient tropical thermostat.

Methods

Experiments

We analyze three types of experiments from the Climate Model Intercomparison Project Phase 6 (CMIP6) archive [50]. The first type consists of two hypothetical CO_2-only experiments: *abrupt 4xCO_2* rise and *1pct* gradual CO_2 rise (1% per year) where CO_2-increases are relative to a pre-industrial level of 280 ppm. The second type has full-forcing experiments: *historical* simulations using prescribed greenhouse gas (GHG) and aerosol emissions (based on observations), as well as two future scenarios, *ssp585* and *ssp353*, which follow possible future GHG and aerosol emission trajectories. The third type of experiments consists of modified historical runs with either historical GHG concentrations prescribed and no aerosols (*hist-GHG*), or prescribed historical aerosol emissions with a constant preindustrial CO_2 level (*hist-aer*). Note that for UKESM1 and MPI-ESM-1-2-HAM, we used the *hist-piaer* (historical with pre-industrial aerosol emission) simulation rather than the *hist-GHG* simulation as the latter was not available. The *hist-piaer* simulation, however, is similar to *hist-GHG* for our purposes since it keeps aerosol emissions constant at the pre-industrial level.

Models

We use a total of 40 CMIP6 models in our analysis. The criterion for including a given model is whether it has at least one ensemble member and 150 years of simulation available for the following experiments: *abrupt4xCO_2*, *1pct*, *pi-Control*, and *historical* (at the time the data was downloaded during a period from March to September 2020). Some models did not have future projected scenarios (Fig 5b), and these models are excluded from that part of the analysis. For the CO_2-only simulations, given the strong forcing signal, we only use one ensemble member per model, but for the historical simulation and future projections, for which the forcing is smaller and therefore natural variability plays a greater role, we include all available ensemble members, which ranges from 1 to 32 (see Fig S1). For Fig 1, however, we use only one ensemble member per model to give equal weight to each model. In addition, a subset of 12 models is used for the second part of the analysis in which we separate the effects of CO_2 and aerosols by analyzing the GHG-only and aerosols-only simulations and comparing them to the full-forcing historical simulations. These 12 models are selected based on the criterion of having at least one ensemble member available for each of the three types of historical simulations – realistic and partial-forcing.

Metrics

We define the Indo-Pacific equatorial temperature gradient as the surface temperature of the Indo-West Pacific region (80ºE to 150ºE, 5ºS to 5ºN, including some Maritime continental land areas) minus the

central-east Pacific (180ºE to 280ºE, 5ºS to 5ºN). Occasionally, we will refer to this gradient as SST gradient or Pacific SST gradient since the inclusion of land has only a minor effect, and since this gradient is typically dominated by east-west SST contrast in the Pacific. All anomalies are calculated relative to either a pi-Control time mean of at least 150 years for the hypothetical CO_2-only experiments, or a historical baseline of 1950-1970 for the historical and ssp scenarios. We chose this particular baseline in order to be able to compare simulations to a period with reliable historical observations.

Declarations

Data availability

CMIP6 data is available at: https://esgf-node.llnl.gov/search/cmip6/. Individual dataset used in this study are available upon request in the event they are temporarily unavailable for download at the above directory.

Code Availability

All plots and analysis are carried out using Python v. 3.4 including the following packages: xarray, numpy, xesmf, pandas, os, matplotlib and cartopy. All code is available upon request.

Acknowledgements

U.K.H is supported by NASA FINESST Fellowship (80NSSC20K1634). A.V.F. is supported by grants from the NSF (AGS-0163807) and NASA (NNX17AH21G), the ARCHANGE project of the “Make our planet great again” program (CNRS, France).

References

1. Clement, A. & DiNezio, P. The tropical Pacific Ocean—Back in the driver’s seat? *Science* **343**, 976–978 (2014).
2. Fedorov, A. V., Burls, N. J., Lawrence, K. T. & Peterson, L. C. Tightly linked zonal and meridional sea surface temperature gradients over the past five million years. *Nat. Geosci.* **8**, 975–980 (2015).
3. Kosaka, Y. & Xie, S.-P. The tropical Pacific as a key pacemaker of the variable rates of global warming. *Nat. Geosci.* **9**, 669–673 (2016).
4. Pierrehumbert, R. T. Climate change and the tropical Pacific: The sleeping dragon wakes. *Proc. Natl. Acad. Sci.* **97**, 1355–1358 (2000).
5. Collins, M. *et al.* The impact of global warming on the tropical Pacific Ocean and El Niño. *Nat. Geosci.* **3**, 391–397 (2010).
6. DiNezio, P. N. *et al.* Mean climate controls on the simulated response of ENSO to increasing greenhouse gases. *J. Clim.* **25**, 7399–7420 (2012).
7. Fedorov, A. V. & Philander, S. G. Is El Niño changing? *Science* **288**, 1997–2002 (2000).

8. England, M. H. *et al.* Recent intensification of wind-driven circulation in the Pacific and the ongoing warming hiatus. *Nat. Clim. Change* **4**, 222–227 (2014).
9. Fedorov, A. V., Hu, S., Wittenberg, A. T., Levine, A. F. & Deser, C. ENSO Low-Frequency Modulation and Mean State Interactions. *El Niño South. Oscil. Chang. Clim.* 173–198 (2020).
10. Hu, S. & Fedorov, A. V. The extreme El Niño of 2015–2016 and the end of global warming hiatus. *Geophys. Res. Lett.* **44**, 3816–3824 (2017).
11. McGregor, S. *et al.* Recent Walker circulation strengthening and Pacific cooling amplified by Atlantic warming. *Nat. Clim. Change* **4**, 888–892 (2014).
12. Andrews, T. *et al.* Accounting for Changing Temperature Patterns Increases Historical Estimates of Climate Sensitivity. *Geophys. Res. Lett.* **45**, 8490–8499 (2018).
13. Dong, Y. *et al.* Intermodel Spread in the Pattern Effect and Its Contribution to Climate Sensitivity in CMIP5 and CMIP6 Models. *J. Clim.* **33**, 7755–7775 (2020).
14. Sohn, B.-J., Yeh, S.-W., Lee, A. & Lau, W. K. M. Regulation of atmospheric circulation controlling the tropical Pacific precipitation change in response to CO 2 increases. *Nat. Commun.* **10**, 1108 (2019).
15. Yeh, S.-W. *et al.* ENSO Atmospheric Teleconnections and Their Response to Greenhouse Gas Forcing. *Rev. Geophys.* **56**, 185–206 (2018).
16. Ceppi, P., Zappa, G., Shepherd, T. G. & Gregory, J. M. Fast and slow components of the extratropical atmospheric circulation response to CO2 forcing. *J. Clim.* **31**, 1091–1105 (2018).
17. Kociuba, G. & Power, S. B. Inability of CMIP5 models to simulate recent strengthening of the Walker circulation: Implications for projections. *J. Clim.* **28**, 20–35 (2015).
18. Plesca, E., Grützun, V. & Buehler, S. A. How robust is the weakening of the Pacific Walker circulation in CMIP5 idealized transient climate simulations? *J. Clim.* **31**, 81–97 (2018).
19. Dong, B. & Lu, R. Interdecadal enhancement of the Walker circulation over the tropical Pacific in the late 1990s. *Adv. Atmospheric Sci.* **30**, 247–262 (2013).
20. Ma, S. & Zhou, T. Robust strengthening and westward shift of the tropical Pacific Walker circulation during 1979–2012: A comparison of 7 sets of reanalysis data and 26 CMIP5 models. *J. Clim.* **29**, 3097–3118 (2016).
21. Meng, Q. *et al.* Twentieth century Walker circulation change: Data analysis and model experiments. *Clim. Dyn.* **38**, 1757–1773 (2012).
22. Hu, S. & Fedorov, A. V. Indian Ocean warming can strengthen the Atlantic meridional overturning circulation. *Nat. Clim. Change* **9**, 747–751 (2019).
23. Zhang, L. *et al.* Indian Ocean Warming Trend Reduces Pacific Warming Response to Anthropogenic Greenhouse Gases: An Interbasin Thermostat Mechanism. *Geophys. Res. Lett.* **46**, 10882–10890 (2019).
24. Clement, A. C., Seager, R., Cane, M. A. & Zebiak, S. E. An ocean dynamical thermostat. *J. Clim.* **9**, 2190–2196 (1996).

25. Liu, Z. The Role of Ocean in the Response of Tropical Climatology to Global Warming: The West–East SST Contrast. *J. Clim.* **11**, 864–875 (1998).
26. Luo, Y., Lu, J., Liu, F. & Garuba, O. The Role of Ocean Dynamical Thermostat in Delaying the El Niño–Like Response over the Equatorial Pacific to Climate Warming. *J. Clim.* **30**, 2811–2827 (2017).
27. Heede, U. K., Fedorov, A. V. & Burls, N. J. Timescales and mechanisms for the Tropical Pacific response to global warming: a tug of war between the Ocean Thermostat and weaker Walker. *J. Clim.* (2020) doi:10.1175/JCLI-D-19-0690.1.
28. Fosu, B., He, J. & Liguori, G. Equatorial Pacific Warming Attenuated by SST Warming Patterns in the Tropical Atlantic and Indian Oceans. *Geophys. Res. Lett.* **47**, e2020GL088231 (2020).
29. Levine, A. F., McPhaden, M. J. & Frierson, D. M. The impact of the AMO on multidecadal ENSO variability. *Geophys. Res. Lett.* **44**, 3877–3886 (2017).
30. Seager, R. *et al.* Strengthening tropical Pacific zonal sea surface temperature gradient consistent with rising greenhouse gases. *Nat. Clim. Change* **9**, 517–522 (2019).
31. Knutson, T. R. & Manabe, S. Time-mean response over the tropical Pacific to increased C02 in a coupled ocean-atmosphere model. *J. Clim.* **8**, 2181–2199 (1995).
32. Vecchi, G. A. & Soden, B. J. Global warming and the weakening of the tropical circulation. *J. Clim.* **20**, 4316–4340 (2007).
33. Erfani, E. & Burls, N. J. The Strength of Low-Cloud Feedbacks and Tropical Climate: A CESM Sensitivity Study. *J. Clim.* **32**, 2497–2516 (2019).
34. Stuecker, M. F. *et al.* Strong remote control of future equatorial warming by off-equatorial forcing. *Nat. Clim. Change* 1–6 (2020).
35. Coats, S. & Karnauskas, K. B. Are simulated and observed twentieth century tropical Pacific sea surface temperature trends significant relative to internal variability? *Geophys. Res. Lett.* **44**, 9928–9937 (2017).
36. Burls, N. J. & Fedorov, A. V. What controls the mean east–west sea surface temperature gradient in the equatorial Pacific: The role of cloud albedo. *J. Clim.* **27**, 2757–2778 (2014).
37. Li, G., Xie, S.-P., Du, Y. & Luo, Y. Effects of excessive equatorial cold tongue bias on the projections of tropical Pacific climate change. Part I: The warming pattern in CMIP5 multi-model ensemble. *Clim. Dyn.* **47**, 3817–3831 (2016).
38. Collins, M. & The CMIP Modelling Groups (BMRC (Australia), C. (Canada), CCSR/NIES (Japan), CERFACS (France), CSIRO (Austraila), MPI (Germany), GFDL (USA), GISS (USA), IAP (China), INM (Russia), LMD (France), MRI (Japan), NCAR (USA), NRL (USA), Hadley Centre (UK) and YNU (South Korea)). El Niño- or La Niña-like climate change? *Clim. Dyn.* **24**, 89–104 (2005).
39. Kohyama, T. & Hartmann, D. L. Nonlinear ENSO Warming Suppression (NEWS). *J. Clim.* **30**, 4227–4251 (2017).
40. Lee, S.-K. *et al.* Pacific origin of the abrupt increase in Indian Ocean heat content during the warming hiatus. *Nat. Geosci.* **8**, 445 (2015).

41. Dong, L., Zhou, T. & Chen, X. Changes of Pacific decadal variability in the twentieth century driven by internal variability, greenhouse gases, and aerosols. *Geophys. Res. Lett.* **41**, 8570–8577 (2014).
42. Takahashi, C. & Watanabe, M. Pacific trade winds accelerated by aerosol forcing over the past two decades. *Nat. Clim. Change* **6**, 768–772 (2016).
43. Zhao, B. & Fedorov, A. The Effects of Background Zonal and Meridional Winds on ENSO in a Coupled GCM. *J. Clim.* **33**, 2075–2091 (2020).
44. Song, X. & Zhang, G. J. Role of Climate Feedback in El Niño–Like SST Response to Global Warming. *J. Clim.* **27**, 7301–7318 (2014).
45. Xie, S.-P. *et al.* Global warming pattern formation: Sea surface temperature and rainfall. *J. Clim.* **23**, 966–986 (2010).
46. DiNezio, P. N. *et al.* Climate response of the equatorial Pacific to global warming. *J. Clim.* **22**, 4873–4892 (2009).
47. Ying, J., Huang, P. & Huang, R. Evaluating the formation mechanisms of the equatorial Pacific SST warming pattern in CMIP5 models. *Adv. Atmospheric Sci.* **33**, 433–441 (2016).
48. Lund, M. T., Myhre, G. & Samset, B. H. Anthropogenic aerosol forcing under the Shared Socioeconomic Pathways. *Atmospheric Chem. Phys.* **19**, 13827–13839 (2019).
49. Watanabe, M., Dufresne, J.-L., Kosaka, Y., Mauritsen, T. & Tatebe, H. Enhanced warming constrained by past trends in equatorial Pacific sea surface temperature gradient. *Nat. Clim. Change* 1–5 (2020) doi:10.1038/s41558-020-00933-3.
50. Eyring, V. *et al.* Overview of the Coupled Model Intercomparison Project Phase 6 (CMIP6) experimental design and organization. *Geosci. Model Dev.* **9**, 1937–1958 (2016).

Figures

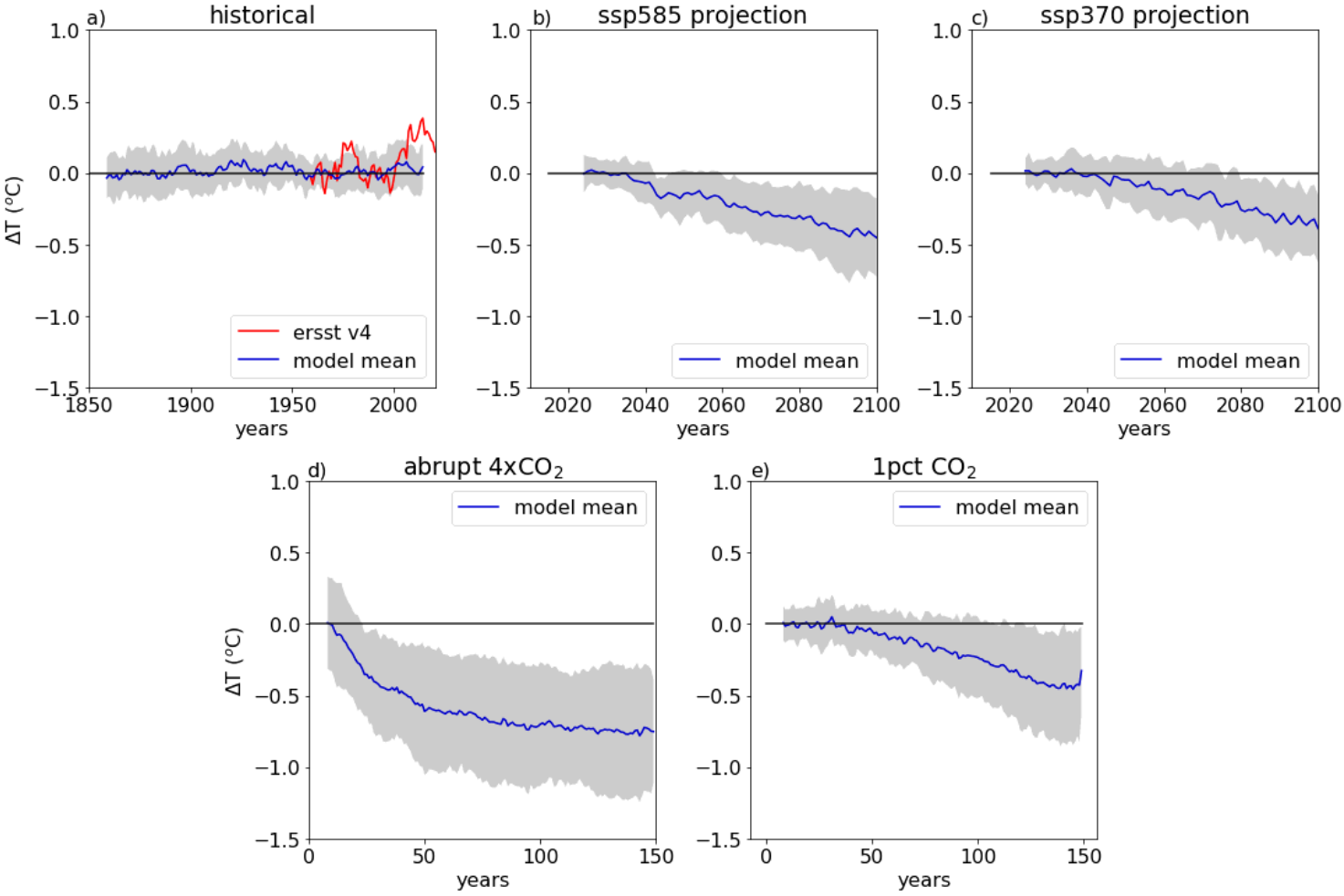

Figure 1

Multi-model-mean evolution of the zonal surface temperature gradient in the equatorial Indo-Pacific Ocean in different experiments. (a) Historical simulations relative to the 1950-1970 base level. The red line indicates changes in the observed SST gradient (errst v4 data) relative to the same base level. (b,c) Future projection scenarios ssp585 and ssp370 relative to the 2015-2025 base level. (d,e) Abrupt 4xCO2 rise and 1pct gradual CO2 rise experiments relative to the preindustrial-control level. In order to weigh each model equally, only one ensemble member per model is included. The shaded area indicates model spread. A ten-year running mean is applied. Positive values indicate the strengthening of the east-west gradient.

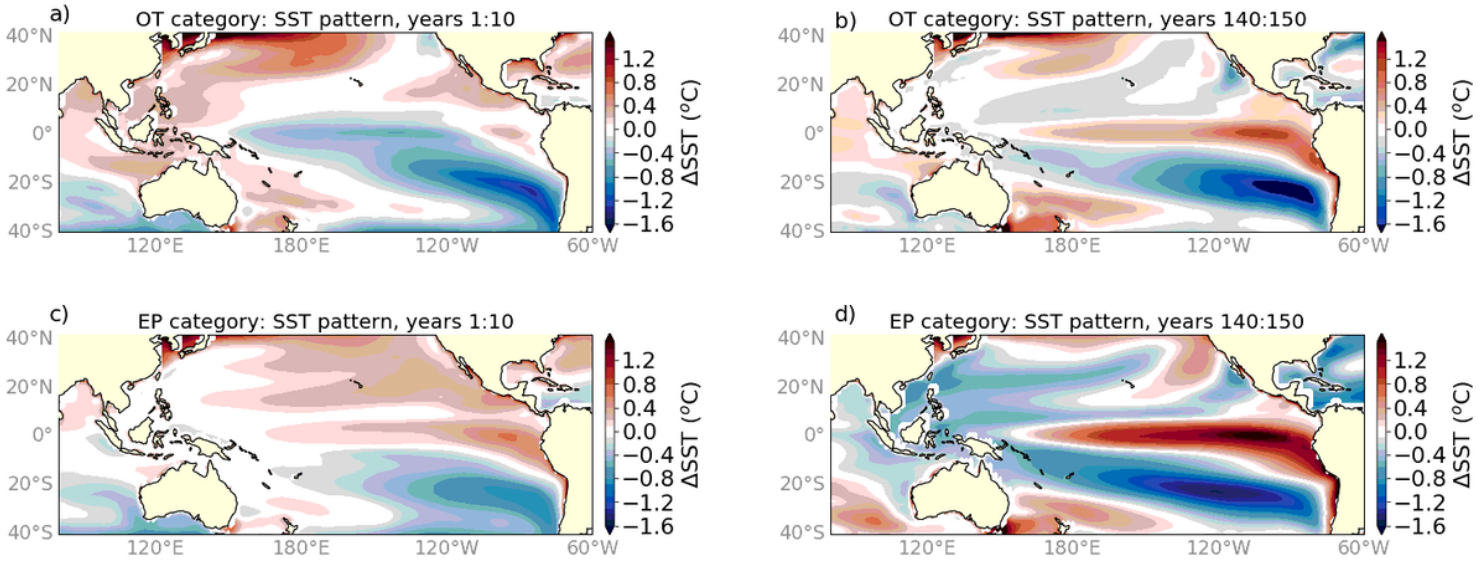

Figure 2

Initial and long-term SST anomaly patterns in the abrupt 4xCO2 experiments. The panel show multi-model-mean anomalies relative to the area mean warming for two model categories based on the structure of the initial response. The ocean thermostat (OT) category contains models with a relative cooling (or lack of warming) in the central and eastern equatorial Pacific in the first 25 years. The eastern equatorial Pacific warming (EP) category contains models with a clear eastern equatorial Pacific warming in the first 25 years. In the long-term (right panels) both categories show a pronounced EP warming pattern but whose strength depends on the type and strength of the initial response. The models assigned to each category are indicated in the legend of Fig. 4. We used 7 and 13 models for the OT and EP categories, respectively. The remaining models fall in between of these two categories. We emphasize that the plot shows SST anomalies computed on top of the mean warming of the tropical Indo-Pacific Ocean.

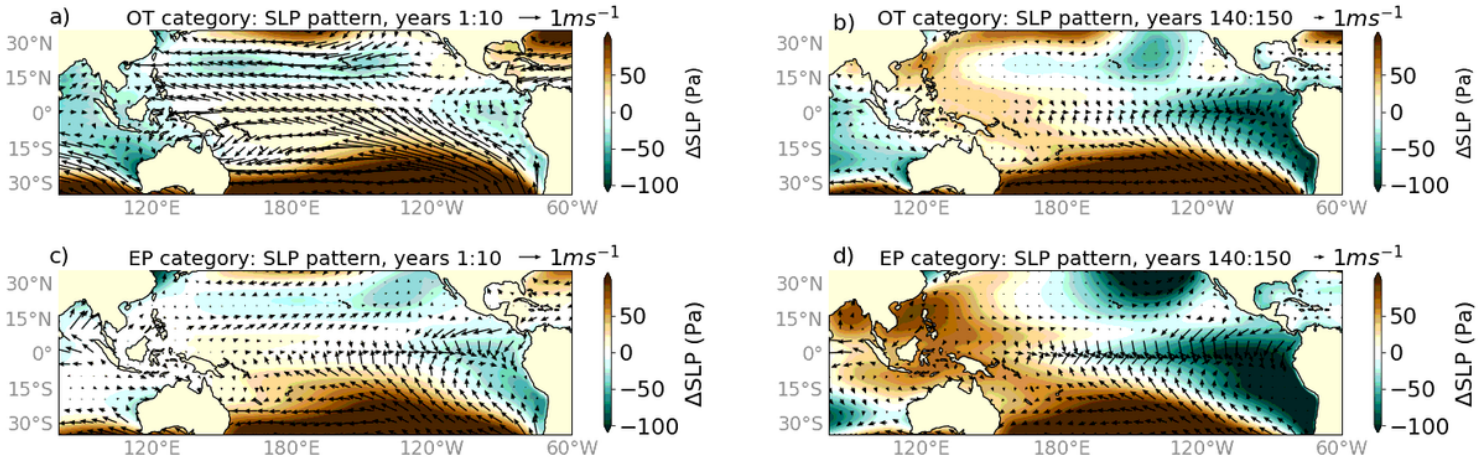

Figure 3

Initial and long-term sea level pressure (SLP) anomaly patterns in the abrupt 4xCO2 experiments. The plot shows SLP anomalies relative to the mean area change for the same two model categories, based on the

initial response (OT and EP), as described in Fig 2. Note the long-term reduction in the east-west SLP gradient associated with the eastern equatorial Pacific warming pattern, indicating the weakening of the Walker circulation.

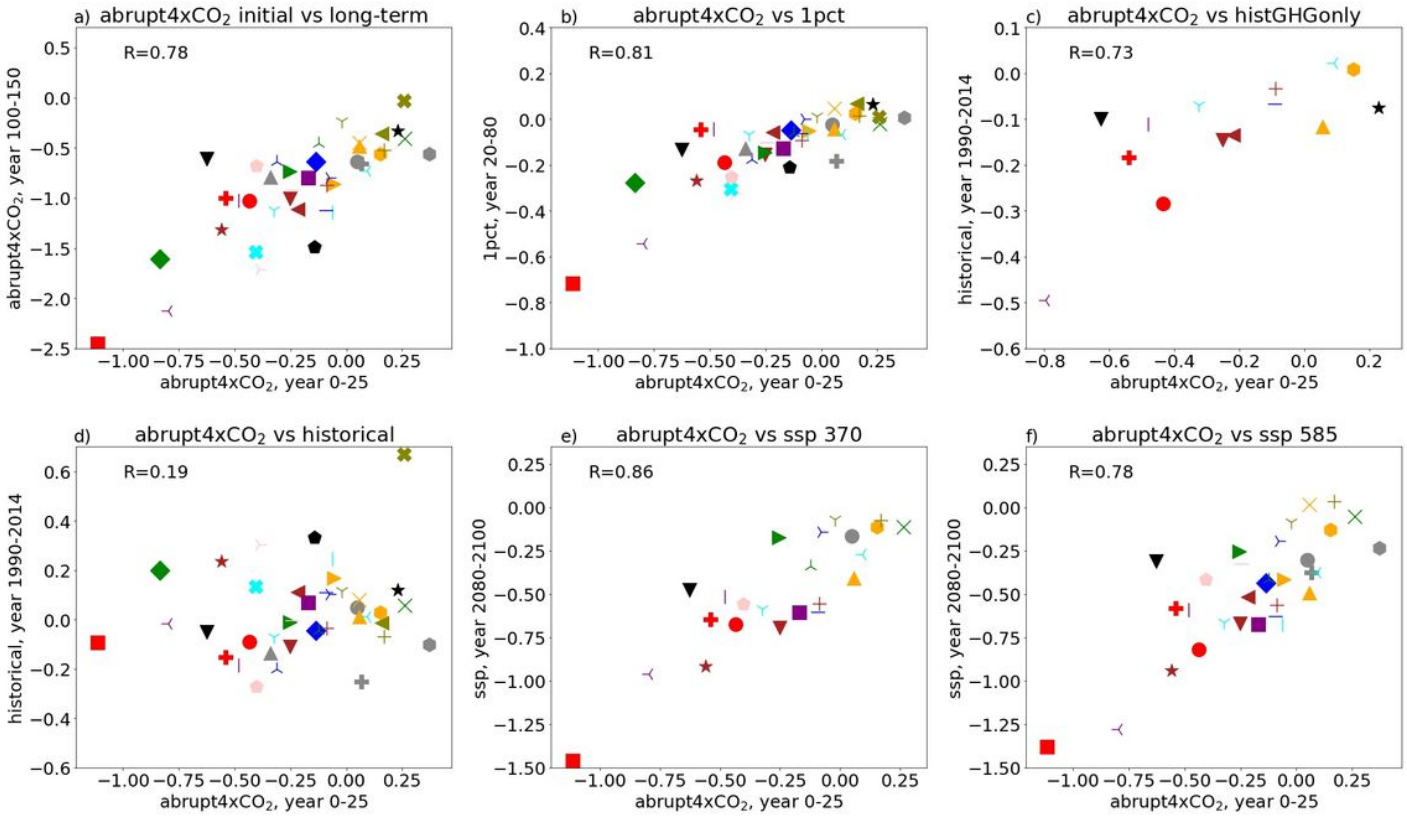

Model name	Marker	Model name	Marker	Model name	Marker	Model name	Marker
ACCESS-CM2 OT	●	CESM2-WACCM-FV2	⬟	GFDL-ESM4*	●	MIROC-ES2L EP	⬟
ACCESS-ESM1-5* EP	▼	CIESM	✚	GISS-E2-1-G*	▼	MIROC6*	✚
BCC-CSM2-MR	▲	CMCC-CM2-SR5 EP	★	GISS-E2-1-H	▲	MPI-ESM-1-2-HAM OT	★
BCC-ESM1*	◀	CNRM-CM6* OT	●	HadGEM3-GC31-LL*	◀	MPI-ESM1-2-LR OT	●
CAMS-CMS1-0 EP	▶	CNRM-CM6-HR OT	+	HadGEM3-GC31-MM	▶	MRI-ESM2*	+
CanESM5* EP	Y	CNRM-ESM2-1 OT	×	INM-CM4-8	Y	NESM3	×
CAS-ESM2-0 EP	⅄	E3SM PE	✖	INM-CM5-0	⅄	NorCPM1 OT	✖
CESM2* EP	⅄	FGOALS-f3-L	◆	IPSL-CM6A*	⅄	SAM0-UNICORN EP	◆
CESM2-FV2 EP	Y	FGOALS-g3*	|	KACE-1-0-G	Y	TaiESM1	|
CESM2-WACCM EP	■	GFDL-CM4	—	MCM-UA-1-0 EP	■	UKESM-0-ll	—

Figure 4

Anomalies in the Indo-Pacific zonal surface temperature gradient in different experiments versus the 4xCO2 initial response: (a) The abrupt 4xCO2 long-term response; (b) the 1pct CO2 20-80 year anomaly; (c) the 1990-2014 anomaly in GHG-only historical simulations relative to pi-Control; (d) the 1990-2014 anomaly full-forcing historical simulation relative to pi-Control; (e,f) the long-term temperature gradient change for the ssp370 and ssp580 scenario (defined as 2080-2100 minus the pi-Control). Each marker+color combination represents one model as described in the legend below the panels. Models marked as OT or EP, respectively, have a clear initial strengthening or weakening of the Indo-Pacific temperature gradient in the first 25 years of the abrupt simulations. Modes that have partial-forcing

experiments available are denoted with an asterisk. Positive values indicate the strengthening of the east-west gradient.

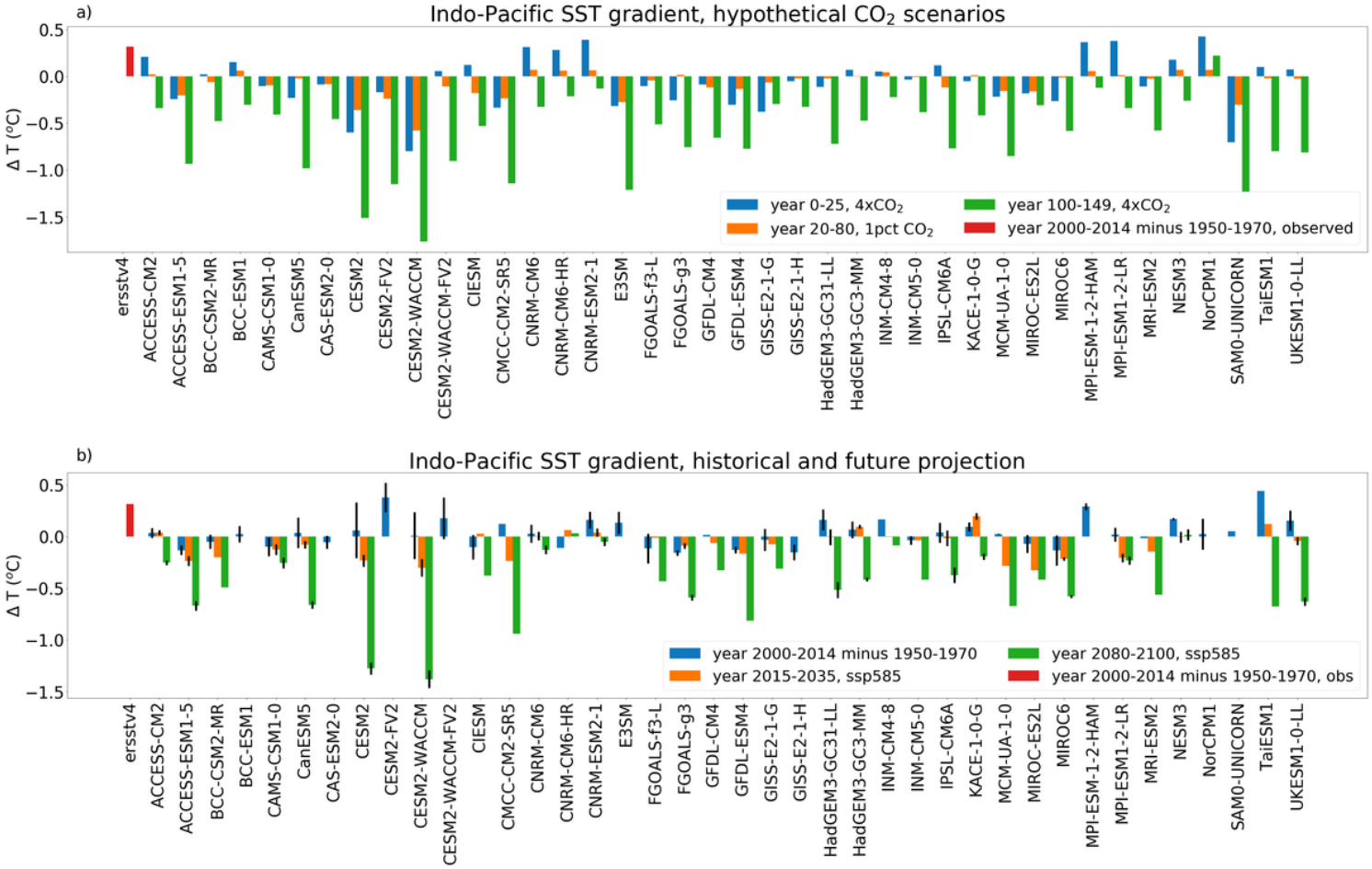

Figure 5

Anomalies in the Indo-Pacific zonal surface temperature gradient in different experiments for each model. This bar chart shows temperature gradient changes for (a) the CO2-only experiments and (b) the full forcing historical and ssp585 simulation. Anomalies in the CO2 experiments are measured relative to a pi-Control baseline. The historical and ssp585 scenario are calculated relative to the 1950-1970 baseline and compared to the observed changes (the red bar). Error bars, when provided, indicate ensemble spread for models that include at least 3 ensemble members.

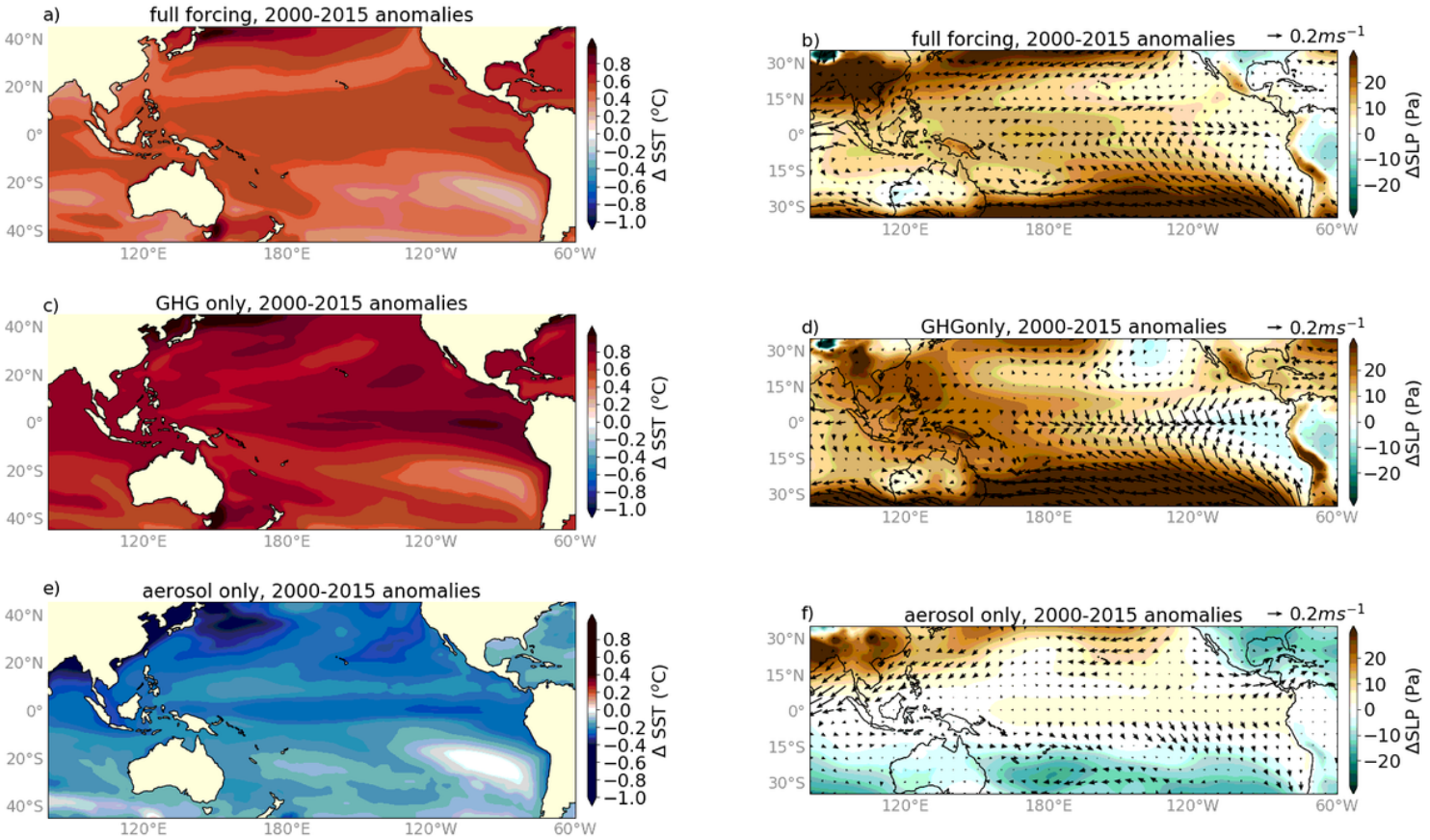

Figure 6

Anomalies in sea surface temperature (SST) and sea level pressure (SLP) in experiments with full or partial historical forcing. The maps show multi-model-mean SST (left) and SLP (right) anomalies for 2000-2014 relative to the 1950-1970 baseline for the three historical experiments: (a,b) full forcing; (c,d) GHG-only and (e,f) aerosols-only. Not that the colorbar for (e) is saturated at -0.5 and 0.5 in order to highlight the pattern of change over the ocean. A subset of 12 models that have all three types of simulations is used (included in Fig. 4c).

Supplementary Files

This is a list of supplementary files associated with this preprint. Click to download.

- EEPsupplementaryfinal.docx